BioNanoScience (2019) 9:672–682
https://doi.org/10.1007/s12668-019-00628-w

Thermodynamics, Kinetics, and Adsorption Properties of Biomolecules onto Carbon-Based Materials Obtained from Food Wastes

Özkan Demirbaş[1] · Mehmet Harbi Çalımlı[2] · Buse Demirkan[3] · Mehmet Hakkı Alma[4] · Mehmet Salih Nas[4] · Anish Khan[5,6] · Abdullah M. Asiri[5,6] · Fatih Şen[3]

Published online: 4 May 2019

Abstract
In this research, adsorption of *Candida rugosa* lipase enzyme (CRLE) onto activated carbon obtained from apple bark was carried out, and the thermodynamic parameters of adsorption process were investigated. The surface structural change of lipase enzyme and activated carbon was studied. The thermodynamic functions such as enthalpy, entropy, Gibbs free energy, and activation energy were investigated in their experimental work. The thermodynamic parameters of ΔG^*, Ea, ΔH^*, and ΔS^* were calculated as − 75.56, 13.42, − 15.29 kJ mol^{-1}, and 202.2 J mol^{-1} K^{-1} for CRLE adsorption, respectively. The experiment results showed that the adsorption process of CRLE on activated carbon is spontaneous and exothermic. The maximum adsorption capacity according to CRLE was 5.5 pH. The maximum adsorption capacity of active carbon was found to be 96.2 mg/g at pH 5.5, 309.5 K, and initial enzyme concentration of 5.0×10^{-3} M. The protein molecules at this point are very stable that is close to the isoelectric point of lipase enzyme. As a result, we can say that the activated carbon can be used as an effective adsorbent for the adsorption of CRLE.

Keywords Activated carbon · Adsorption · Lipase enzyme · Thermodynamic parameters

1 Introduction

Carbon-based materials are being used for a variety of applications such as catalysts, sensors, and adsorption [1–15]. The use of any support molecule of biomolecules in adsorption processes has been extensively evaluated in previous studies [16–24]. The lipase enzyme, a member of the hydrolase class, is an esterase capable of hydrolyzing to glycerol and fatty acids [25]. Lipase enzymes can be converted into esters by hydrolysis under certain conditions in a non-aqueous environment [26]. The immobilized enzymes molecules have higher stability and activity than pure enzymes in the reaction medium [27, 28]. In recent years, immobilization techniques have been extensively carried out [29]. During adsorption processes, some covalent bonding and physical interactions occur. The physical adsorption and enzyme binding in the immobilization process are directly related to surface structure [30]. So, the lipase enzyme immobilization takes place via hydrophobic interaction between the support and the enzyme [31]. Enzymes have protein structures, and proteins are affected by the conditions of the medium such as pH, ionic strength, protein concentration, and buffer solution state. For this reason,

✉ Mehmet Salih Nas
mehmet.salih.nas@igdir.edu.tr

✉ Anish Khan
anishkhan97@gmail.com

✉ Abdullah M. Asiri
aasiri2@kau.edu.sa

✉ Fatih Şen
fatih.sen@dpu.edu.tr

[1] Department of Chemistry, Faculty of Science and Literature, University of Balikesir, Balikesir, Turkey

[2] Tuzluca Vocational High School, Igdir University, Igdir, Turkey

[3] Sen Research Group, Department of Biochemistry, Faculty of Arts and Science, Dumlupınar University, Evliya Çelebi Campus, 43100 Kütahya, Turkey

[4] Department of Environmental, Faculty of Engineering, University of Igdir, Igdir, Turkey

[5] Chemistry Department, Faculty of Science, King Abdulaziz University, 80203, Jeddah 21589, Saudi Arabia

[6] Center of Excellence for Advanced Materials Research, King Abdulaziz University, 80203, Jeddah 21589, Saudi Arabia

protein adsorption studies have recently been extensively studied on experimental conditions [32–35]. The activated carbon is widely used in adsorption processes to remove pollutants from wastewater. However, the activated carbon in the market is expensive. So in recent years, it has been started to produce low-cost activated carbons, which can be renewed and abundant especially for the treatment of wastewater. Recently, various studies have performed to obtain activated carbon from fruit stones and nutshells [36], cassava peel [37], palm-tree cobs [38], olive stones [39], plum kernels [40], bagasse [41], rice husks [42], date pits [43], and jute fiber [44]. There are few studies in the literature on the immobilization of pure lipase enzyme, and the use of pure enzymes is not economical. The use of the immobilized pure enzyme can be used easily and repeatedly. Because of these advantages, we performed lipase enzyme immobilization study. In Turkey, apple plants are abundant and are used extensively in many areas of industry. As a result of the use of apple fruit, large amounts of crust appear as garbage. The evaluation of these shells as an active carbon source is very economical. Lipases are used to catalyze the hydrolysis, alcoholisation, acidification, and amidolysis of petroleum products. For these reasons; lipases have the potential to be widely used in many areas such as biochemistry, food technologies, and chemical industries. The present work aimed to reveal the adsorption process results of CRLE on activated carbon and determine its activation parameters.

2 Experimental

2.1 Materials and Methods

The lipase enzyme (*Candida rugosa*) used in the study was purchased from Sigma. The solvents and chemicals were purchased from Merck AG (Darmstadt, Germany). All chemicals used in the study were of analytical grade. The activated carbon used in the study was synthesized from the shells of fruit. Turkey is the fifth in the world in terms of apple production area and ranks third in terms of the amount of production. Considering the production amount, Turkey meets approximately 4% of the world's apple production [45]. The SEM (SCM 5000) was used to clarify the microstructural and morphological structure of the activated carbon sample. The water was passed from Milli-Q system and distilled two times. The elements contained in the activated carbon sample and the percentages of these elements are given in Table 1. The BET N_2(Micromeritics Flow Sorb II 2300) was used to investigate the specific surface area of the activated carbon, and BET analysis of the activated carbon was given in Table 2. The TGA was obtained simultaneously using a PerkinElmer instrument. The FTIR device was used to compare the initial and final organic functional contents of the support material used in the adsorption process Table 1.

Table 1 Elements content of activated carbon

Elements	Amount (%)
C	58.1
O	10.14
S	6.88
Cl	12.76
Al	2.61
Cu	5.59
Si	2.71
Others	1.12

2.2 Adsorption Studies

The adsorption of CRLE on activated carbon obtained from apple bark was studied in a typical water tank. A certain amount of active carbon was added to 100 ml enzyme solution to a 500 ml Erlenmeyer swollen working set. The mixture was shaken rapidly at a predetermined temperature and for the desired time in an unmixed shaker. The enzyme samples taken in the working set were centrifuged for 7 min at 12.000 rpm, and then the supernatant was removed from the centrifuge tube and measured on a UV-vis spectrophotometer. Analysis values were measured at 208 nm wavelength. The adsorption efficiency of CRLE on activated carbon was calculated using the following equation [46].

$$Y(\%)=100\ \frac{(\mathrm{Co}-\mathrm{Ci})}{\mathrm{Co}} \tag{1}$$

where; Co is the first pure concentration (g/L) of the stock enzyme solution prepared, and Ci is the final liquid phase concentrations at any time of the biomolecule solution. The parameters such as initial enzyme concentration (100–350 mg/l), solution pH (5.5–9), and temperature (288–318 K) were investigated at a specific time interval for the adsorption process. In the experimental study, the amount

Table 2 Some physicochemical properties of activated carbon

Parameters	Value
Color	Black
pH	4.85
Specific surface area ($m^2\ g^{-1}$)	
Particle size (mesh)	325
Single point specific surface area	9.593e + 02 $m^2\ g^{-1}$
Multipoint specific surface areas	9.616e + 02 $m^2\ g^{-1}$
Langmuir surface area	1.489e + 03 $m^2\ g^{-1}$

adsorbed enzyme at the moment of equilibrium was calculated with the following equation [47].

$$q_t = \frac{(C_0 - C_e)V}{m} \quad (2)$$

where,

C_0 and C_e (mg/l) are lipase enzyme concentration for the initial and the equilibrium states, respectively. q_t (mg/g) is the amount of adsorption at any time and m (g) is the mass of the activated carbon Fig. 1.

3 Results and Discussion

3.1 Evaluating the Characterization Studies for Adsorption Materials

The balance in the blue curve in Fig. 4a was taken into consideration. The amount of *Candida rugosa* lipase on the activated carbon surface was approximately found to be 0.17 m mol/g. FTIR, SEM, and TGA measurements were performed to evaluate chemical and physical properties of activated carbon, *Candida rugosa* lipase, and immobilized activated carbon. The activated carbon, lipase enzyme, and immobilized enzyme samples were investigated using a scanning electron microscope (SEM) device to determine morphological and surface properties as indicated in Fig. 2a. Untreated surface clusters (Fig. 2b) before being treated with activated carbon can be seen with some flat particles in the porosity. We can see that the pores become more flattened and the clay surface become smaller after treated with enzyme molecules. Analysis of activated carbon surfaces because of adsorbed lipase enzyme was carried out in three-dimensional level by SEM. Figure 2 shows the activated carbon structures

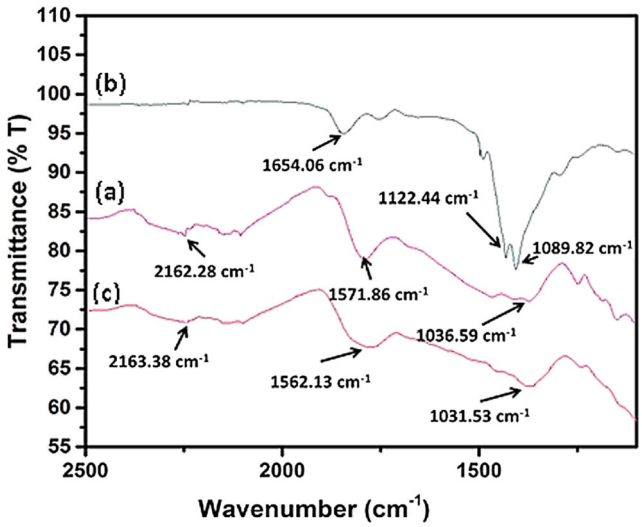

Fig. 1 FTIR spectra of AC (a), LE (b), and lipase enzyme adsorbed activated carbon (LE-AC) (c) after 120 min

adsorbed by the lipase enzyme for 2 h and at 308 K. The surface shape and structure grain of activated carbon, lipase, and lipase adsorbed on activated carbon are different from each other, and these differences are seen in Fig. 2. As seen in Fig. 2a and b, the mean size of grain and pores of surface on activated carbon and lipase can be seen evidently. However, the mean size of grain and pores of surface of the activated carbon adsorbed lipase have been listed in Fig. 2c. These morphological changes are seen in SEM images as given in Fig. 2c. Figure 3a,b,c show the thermal gravimetric analysis (TGA) profile of the activated carbon, lipase enzyme, and immobilized enzyme samples. The TGA analysis was carried out to analyze the effect of heat on the surface structure of activated carbon and enzyme molecules. The activated carbon (19.2%), the lipase enzyme (6.3%), and the lipase enzyme adsorbed on the activated carbon (16.9%) have been severely mass lost between 25 and 100 degrees. This is a consequence of the dehydration phase, which corresponds to the removal of adsorbed and hydrated water. In Fig. 1c, activated carbon mineral gave two peaks in band 1571 cm^{-1} and band 2163 cm^{-1}. This situation is mainly associated with (C=C stretching) and phenolic and carboxylic groups (C-OH and O–H), respectively. In the same way, the peaks of activated carbon mineral in this range have been observed to work differently [48, 49]. It consists of three bands in the FTIR absorption spectrum of the pure lipase enzyme, which is caused by peptide group vibrations in the 1800–1300 cm^{-1} spectra interval [50]. In Fig. 1c, activated carbon mineral gave two peaks in band 1571 cm^{-1}, band 2163 cm^{-1}, and 1036 cm^{-1}. This situation is mainly associated with (C=C stretching) and phenolic and carboxylic groups (C–OH and O–H), respectively. Fig. 1c shows the FTIR spectra of activated carbon, the bands at 2162 cm^{-1}, and 1036 cm^{-1} are related to the C–OH, O–H, and C–O, C–N bond vibrations, indicating the presence of various functional groups. Furthermore, C=C aromatic skeletal stress of carbon was observed as 1640 and 1444 cm^{-1} bands [51]. In another study, a new peak was detected at 1124 cm^{-1}, which could be assigned to C=S stretching [51]. Due to the C–O stretching vibrations, the amid band in 1654 cm^{-1} peaked at the maximum point and the N–H bending, which was due to the C–N stretching vibration, peaked at the maximum amide II band at 1541 cm^{-1}. Finally, the amide III band (1400 to 1200 cm^{-1}) is the result of N–H bending, C–C and C–N stretching vibrations. Amide I and amide II the bands have very sensitive properties because the proteins are in secondary structure. These proteins lose their structure after a certain temperature in the FTIR spectrum [52, 53]. But the amide III band is much more complex. For this reason, the amide III band is bound to the force field, to the structure of the side chains, and to the hydrogen bonding [52]. The pure lipase enzyme peaked at 1654 cm^{-1} originating from the C–O stretching vibration Fig. 1b. Also, it can be assumed that the intensity of the absorption band of the

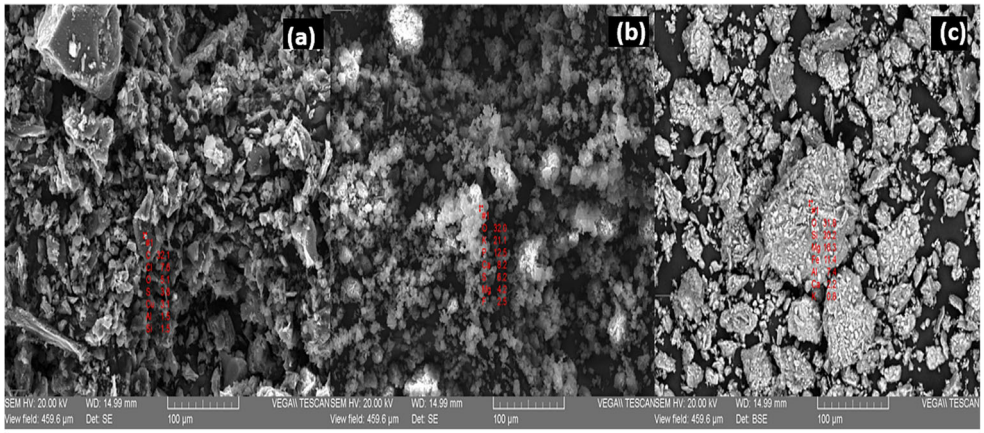

Fig. 2 SEM microphotographs of AC (**a**), LE(**b**), and lipase enzyme adsorbed activated carbon (LE-AC) (**c**) after 120 min

activated carbon was increased with the amide I band. Both the experimental data and the TGA results clearly show the change in the physical meaning of the lipase enzyme adsorbed on activated carbon.

3.2 Effect of Changing Concentration and Ionic Strength

The stock enzyme solutions prepared at different ratios in certain constant parameters were prepared to determine the concentration effect. An increase in the value of the absorbance per unit time was determined depending on the increasing enzyme concentration in the result. Empty areas on the surface at low concentration are active but begin to decrease as the concentration of the enzyme molecule increases. On the other hand, we can finally say that the support is closely related to the increase in the adsorption capacity of the support material due to the increase in propulsive forces for mass transfer. The presence of ionic solution had significantly influenced the adsorption rate of CRLE. As shown in Fig. 4b, the increase in the amount of sodium phosphate salts resulted in an increase in the amount of adsorption. The addition of sodium phosphate in the adsorption process causes two influences. In the first case the amount of salt added to solution medium decreases the interaction by entering between activated carbon and protein molecules. In the latter case, the surface contact area between activated carbon and protein molecules increases with the increase of phosphate salt. It can be said that the increase in the adsorption capacity of the adsorption process of these two processes in the second case is a more dominant effect. Similar results are observed in adsorption of biomolecules and dyestuffs on the clay surface [50, 52–55].

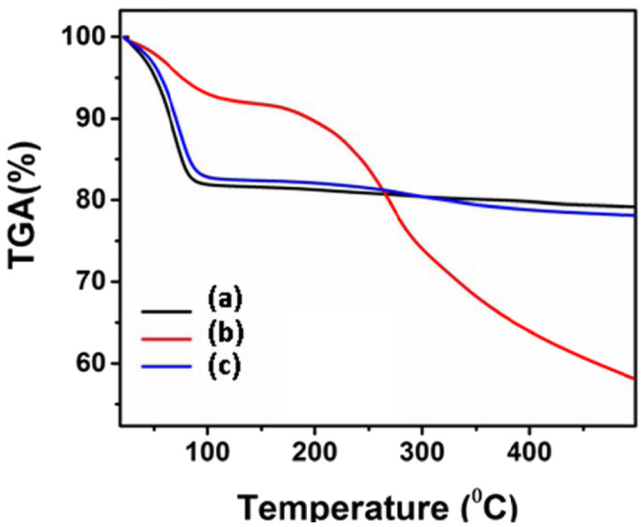

Fig. 3 Thermal gravimetric analyses of AC (a), LE (b) and lipase enzyme adsorbed activated carbon (LE-AC) (c) after 120 min

3.3 Effect of Solution pH Value

The pH value of the solution is considerably influential in adsorption studies, especially in the adsorption process. The presence of functional groups on enzyme molecules has a great effect on the magnitude of electrostatic charges for control purposes. Thus, the pH increase of the solution increases the concentration of the hydroxyl groups in the solution which increases the numerical volume of the negatively loaded regions so that the adsorption interaction between the enzyme and the support material becomes difficult. The effect of solution pH to CRLE adsorption on activated carbon was evaluated at a pH of 5.5 to 9. The results obtained from the experiments done at different PH are given in Fig. 5. As the pH value increases, the yield decreases in adsorption amount. The zero load point, in which hydroxyl and proton ions are equivalent, has an important effect on the pH effect, especially in protein adsorption processes [56]. Because the net charge is zero at the isoelectric point in which enzymes or proteins has a very stable structure. Enzymes are more active at this point or near these points, preserving their three-dimensional structure. But these structures will start to decompose stable values

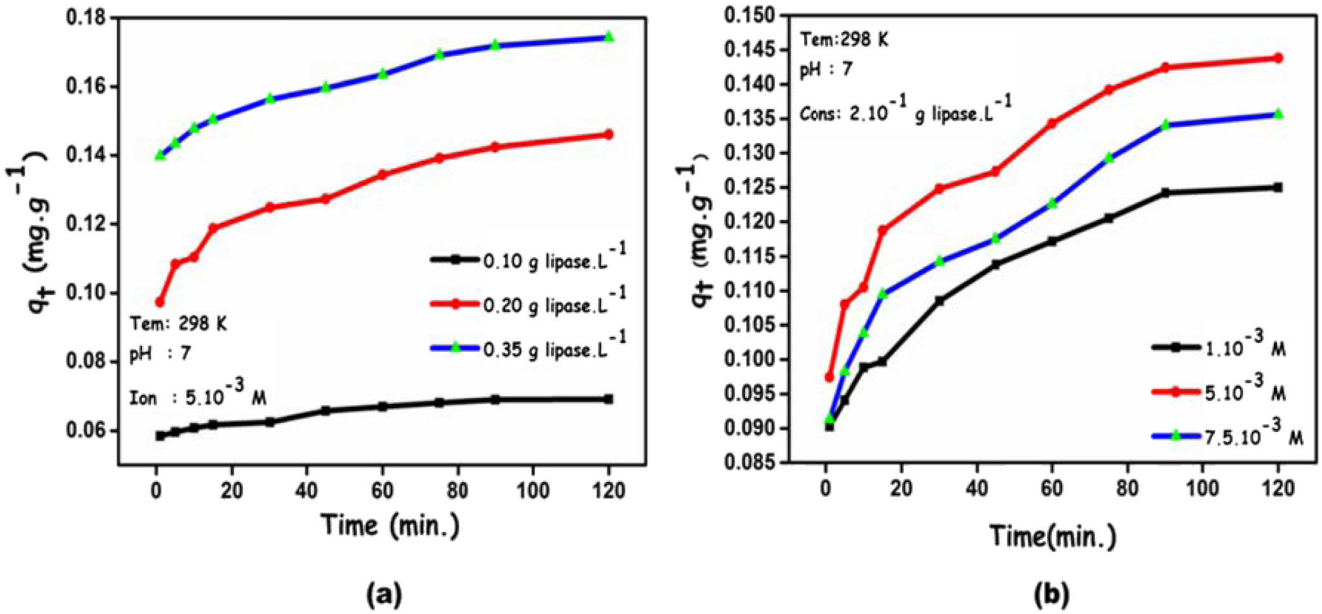

Fig. 4 The effect of initial enzyme concentration (**a**) and ionic strength (**b**) to the adsorption rate of lipase enzyme on activated carbon

below or above the isoelectric point. This situation adversely affects the amount of adsorption [57]. Loads on the surface of proteins that are biomolecules are not homogeneous. When the pH of the solution changes, the charge on the protein surface changes. The isoelectric point of enzyme molecules in adsorption studies is very important. The net charge at the isoelectric point is zero, and each enzyme has a certain isoelectric pH point. At this isoelectric point, the enzymes are more stable and more active [58]. The pH values below the isoelectric point of the CRLE are usually positively charged, and the pH values above isoelectric point of the CRLE are usually negatively charged [59]. In fact, in this study, the maximum adsorption capacity according to CRLE was found at a pH of 5.5. The similar results for some biomolecules adsorption on the surface of krill clay have been evaluated by Demirbas. O [60] (Fig. 6).

3.4 Adsorption Kinetic Studies

CRLE adsorption effect was investigated depending on the contact time on the activated carbon obtained from the apple husk and as a result, increased contact time until reaching

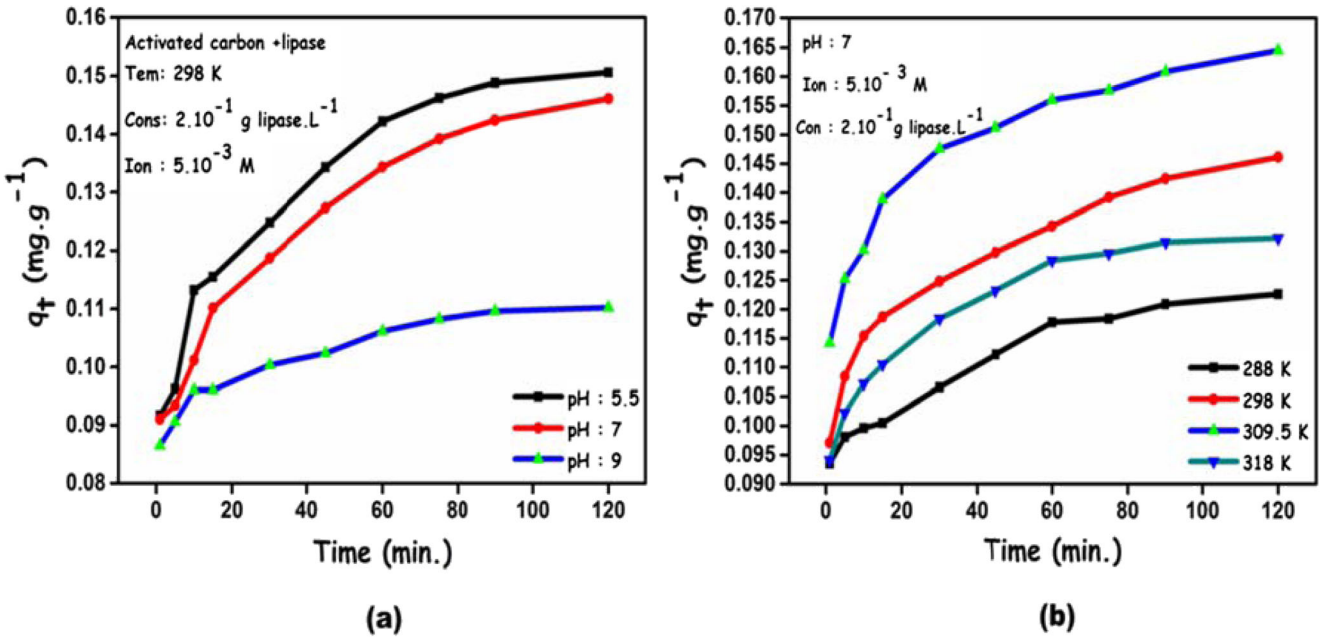

Fig. 5 The effect pH (**a**) and temperature (**b**) to the adsorption of lipase enzyme on activated carbon

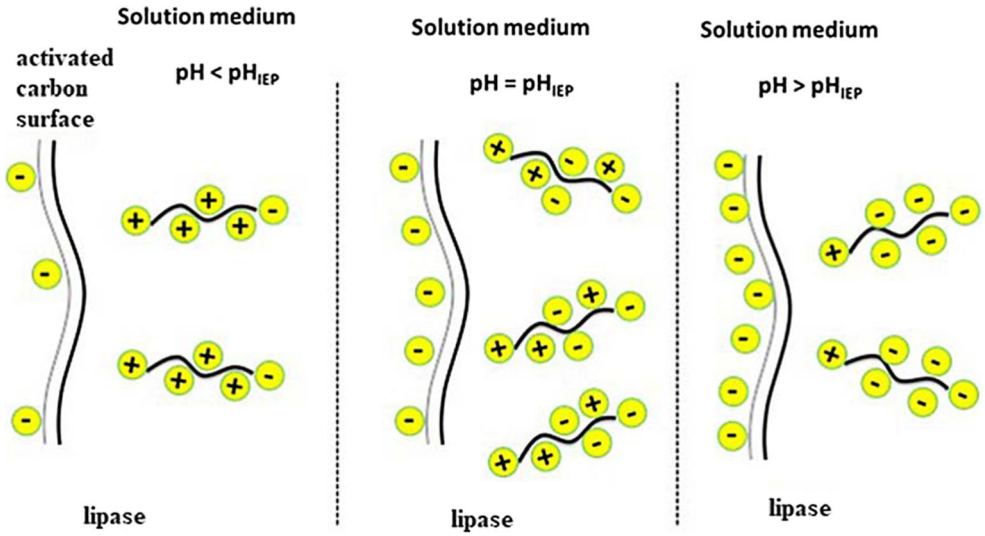

Fig. 6 Effect on the activated carbon surface at different pH medium of the lipase enzyme

equilibrium increased absorbance value observed. Pseudo-first-order, pseudo-second-order and intra-particle diffusion kinetics equations were investigated in order to understand the mechanism and thermodynamics of the adsorption process. The pseudo-first-order equation is given as follows;

$$\frac{dq_t}{dt} = k(q_e - q_t) \tag{3}$$

The equation for this model [60–62] is given below. In the Eq. (3) t (min.) is the time, k_i is the constant of rate, q_e and q_t the first and last quantities (mol g^{-1}) of lipase enzyme, respectively.

$$\log(q_e - q_t) = \log q_e - \frac{k_1 . t}{2.303} \tag{4}$$

The values of q_e and k_1 are found from the slope and the intersection of linear plot of log (q_e–q_t) versus time (t) is specified in Table 3. The pseudo-second-order equation is given as follows [63].

$$\frac{t}{q_t} = \frac{1}{k_2 {q_e}^2} + \frac{t}{q_e} \tag{5}$$

where k_2 is the velocity constant of the reactance. The k_2 represents the rate constant of the reaction. The values q_e and k_2 are obtained as shown in Table 4 at slope values and t/q_t and t cutoff point. In-particle diffusing work generally takes place in three stages: (1) by initially transporting the absorbed material from the delimiting film to the outer surface; (2) then adsorbed to any region on the surface; (3) with the intra-particle diffusion of the enzyme molecule into the adsorption region of a pore diffusion process (Fig. 7) In this case, the slowest of the three steps is considered as the step controlling

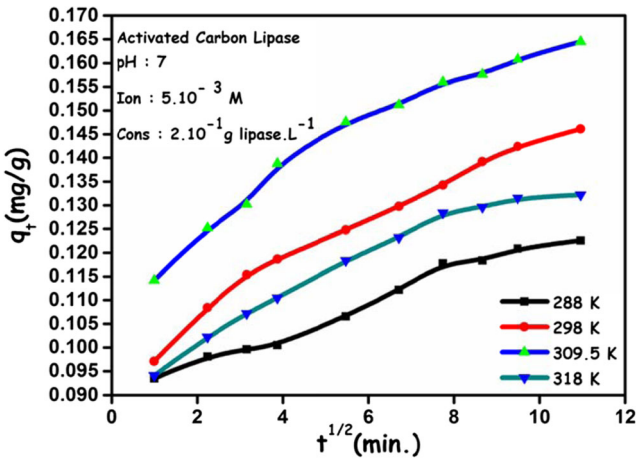

Fig. 7 Intra-particle diffusion plots for different temperature

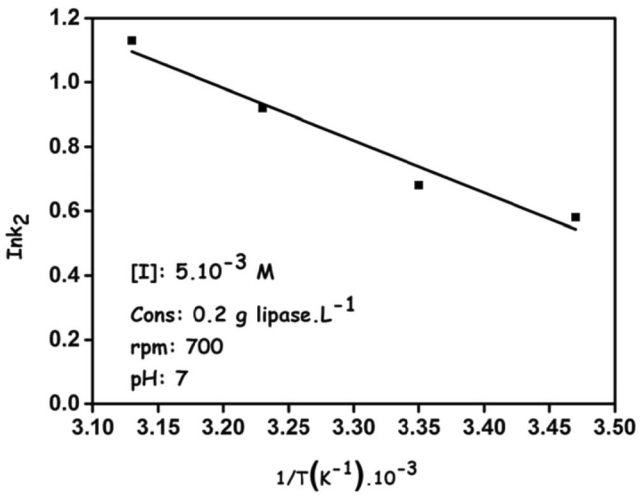

Fig. 8 Arrhenius plot for the adsorption of lipase enzyme on activated carbon

Table 3 Kinetic data calculated for adsorption of lipase enzyme on activated carbon

Kinetic models											
Parameters						Pseudo-second-order					
T/K	Conc (mol $L^1 \times 10^1$)	pH	Stirring speed (rpm)	[I] (mol L^1) 10^2	Pseudo first-order R^2	q_e(cal.) (mg g^{-1})	q_e(exp.) (mg g^{-1})	k_2(g mg^1 min^{-1})	R^2	h(mol min^{-1} g^{-1})	$t_{1/2}$ (min).
288	2	7	700	5	0.95	0.128	0.126	1.8085	0.99	0.2278	4.389
298	2	7	700	5	0.95	0.1461	0.147	1.937	0.99	0.2847	3.512
310	2	7	700	5	0.97	0.1645	0.165	2.4855	0.99	0.4101	2.4384
318	2	7	700	5	0.91	0.1332	0.134	3.0449	0.99	0.408	2.4509
298	1	7	700	5	0.9	0.0692	0.07	8.447	0.99	0.5913	1.6912
298	2	7	700	5	0.95	0.1461	0.147	1.937	0.99	0.2847	3.512
298	3.5	7	700	5	0.95	0.1742	0.175	2.555	0.99	0.4471	2.2365
298	2	5.5	700	5	0.99	0.1506	0.154	1.6438	0.99	0.2531	3.9503
298	2	7	700	5	0.95	0.1461	0.147	1.937	0.99	0.2847	3.512
298	2	9	700	5	0.94	0.1102	0.111	4.8397	0.99	0.5372	1.8615
298	2	7	700	2.5	0.9	0.125	0.126	2.6746	0.99	0.337	2.9674
298	2	7	700	5	0.95	0.1461	0.147	1.937	0.99	0.2847	3.512
298	2	7	700	7.5	0.96	0.1414	0.141	1.5635	0.99	0.2205	4.5361

the reaction. The probability of intra-particle diffusion is obtained by utilizing the intra-particle diffusion model [62–64]. The intra-particle diffusion model is regarded as a function that changes depending on the square root of the time term, as expressed in the equation below.

$$q_t = k_{id} t^{1/2} + C_i \quad (6)$$

where q_t is the amount adsorbed at a given time. The k_{id} is the particle velocity constant mg/g $min^{1/2}$). while C_i is the intercept at stage i and defines the thickness of the boundary layer in the adsorption process. The larger C_i values indicate the effect of the boundary layer on the diffusion of the material during the adsorption process. The intra-particle diffusion rate constant is expressed by the slope of the linear curve of q_t versus $t_{1/2}$, and the values are shown in Table 3. It controls

Table 4 Kinetic data calculated for adsorption of lipase enzyme on activated carbon

Mechanism of adsorption									
Mass transfer					İntra-particle diffusion				
Parameters T/K	Conc. (mol L^{-1}). 10^2	pH	Stirring speed (rpm)	[I] (mol L^1) 10^2	R^2	$k_{int.1}$ mg g^{-1} $min^{-1/2}$	R_1^2	$k_{int.2}$ mg g^{-1} min^{-1}	R_2^2
288	2	7	700	5	0.83	0.449	0.99	0.159	0.91
298	2	7	700	5	0.85	0.611	0.96	0.361	0.96
310	2	7	700	5	0.82	0.79	0.99	0.309	0.81
318	2	7	700	5	0.79	0.506	0.99	0.132	0.89
298	1	7	700	5	0.9	0.12	0.97	0.044	0.94
298	2	7	700	5	0.85	0.611	0.96	0.361	0.96
298	3.5	7	700	5	0.92	0.376	0.99	0.323	0.86
298	2	5.5	700	5	0.84	0.845	0.99	0.256	0.96
298	2	7	700	5	0.85	0.611	0.96	0.361	0.96
298	2	9	700	5	0.83	0.273	0.96	0.081	0.96
298	2	7	700	2.5	0.86	0.421	0.99	0.246	0.85
298	2	7	700	5	0.85	0.611	0.96	0.361	0.96
298	2	7	700	7.5	0.91	0.622	0.99	0.465	0.99

Table 5 Thermodynamic function data obtained by adsorption of BSA on the activated carbon surface

T/K	ΔG kJ/mol	Parameters Ea kJ/mol	Δ*H* kJ/mol	Δ*S* j/K.mol
288	− 73.53			
298	− 75.56			
309.5	− 77.88	13.42	− 15.2994	202.22
318	− 79.60			

the in-particle diffusion phenomenon of ions in the adsorbent. It can be deduced from all the kinetic data obtained that the value of the regression coefficient calculated from the graph referring to the kinetic model from the pseudo-second-order is found to be the highest. It has been found that the adsorption kinetics of CRLE on activated carbon obtained from the apple bark is best defined by the pseudo-second-order model.

3.5 Temperature Effect

The temperature effect on the adsorption of CRLE ions onto the activated carbon apple bark used as the adsorbent was investigated. In the adsorption of CRLE molecules, temperature effect can be used as an important function. Adsorption experiments of CRLE on activated carbon were performed at different temperature (288, 298, 309.5, and 318 K) are given in Fig.5b. The adsorption of CRLE on the surface of activated carbon is increased by the increase of the temperature. However, maximum adsorption yield was obtained at 309.5 K. The CRLE molecules are very sensitive to temperature. The structure CRLE enzyme begins to deteriorate at high temperatures. Adsorbing zones lose their activity at high temperatures. Therefore, interaction of CRLE molecules with support materials is insufficient at very high temperatures which leads to a reduction in the adsorption effect. Additionally, Mohd Basyaruddin Abdul Rahman and his colleagues [65] stated that lipase enzyme molecule adsorption on activated carbon results in maximum activity between 303 and 313 K. In this study, the maximum adsorption value for lipase enzyme adsorption was found to be 309.5 K (Fig. 5b). When the temperature drops below 303 K, an enhancing of reactant viscosity occurs. At this stage, the reactant diffusion is reduced, and this leads to a decrease in activity of adsorption process [66]. A decreasing of adsorption of the enzyme can occur due to the structure of enzyme above of 313 K. Or this may be due to the attenuation of the electrostatic interaction between activated carbon and lipase enzyme at high-temperature (Fig. 8).

The experiments performed at different temperatures showed that the adsorption does not occur chemically but physically. Similar results have been found in other researchers in sorption processes [67–70]. The protein molecules are usually very active in the temperature range (308.5–310 K). In parallel with his work, Vecchia RD et al. found that the maximum adsorption of the immobilized lipase enzyme with different support materials was found to be (310 K) [55]. Pronk. et al. do a study immobilization *Candida rugosa* lipase on hollow fiber membrane. The optimum conditions for enzyme immobilization are obtained at these near temperature values [71]. Montero et al., Xu et al., and various investigators have reported an optimal temperature for the lipase enzyme of 310 K [71–73].

The standard Gibb's energy is described in this case by:

$$\Delta G^{o} = -RT \ln K_c \tag{7}$$

where K_c refers to the degree of movement of the support material in the solution and the adsorbent retention ability of the support material [74]. The K_c values are obtained from the equation below.

$$K_c = \frac{q^2}{C_e} \tag{8}$$

where q_e is the amount adsorbed at equilibrium and C_e is the concentration of the enzyme in the solution. The thermodynamic parameters such as the change of the standard enthalpy ($\Delta H°$) and the standard entropy ($\Delta S°$) are determined using the Van't Hoff equation [75].

$$\ln Kc = \frac{\Delta S^0}{R} - \frac{\Delta H^0}{RT} \tag{9}$$

The $\Delta H°$ and $\Delta S°$ values were found by taking the slope of the Van't Hoff relative to ln K_c of 1/T [79]. The results are

Table 6 Some studies related to the adsorption of *Candida rugosa* enzyme on some supporting materials and their maximum amount qe(max.) of enzymes

Enzymes	Supported materials	Max. q_e (mg/g)	References
Candida rugosa	NanoZrO_2-A	23	[76]
Candida rugosa	hydrophobic resin	134	[77]
Candida rugosa	*n* ± type porous silicon at high oxidation (HO-Psi)	47	[78]
Candida rugosa	*n* ± type porous silicon at low oxidation (LO-Psi)	140	[78]
Candida rugosa	Cellulose nanofibrous membrane	41.02	[65]
Candida rugosa	Magnetic silica aerogel	81.7	[45]
Candida rugosa	Activated carbon	96.2	Our study

shown in Table 5. The negative value of $\Delta H°$ indicates that the adsorption process is exothermic (Fig.6). The values of $\Delta G°$ at the whole temperatures were found to be negative that indicates the adsorption process of CELL on activated carbon is spontaneous.

Some studies related to the adsorption studies of some support materials with *Candida rugosa* enzyme are found in the literature are given in Table 6. When the results of the studies in the literature are compared with the results of our study, it can be seen that the result (96 mg/g) is of remarkable value. Therefore, activated carbon obtained from the apple shell can be used as a supporting material in adsorption studies.

4 Conclusions

The activated carbon as support material in adsorption processes is strikingly effective for adsorbing CRLE molecules from aqueous media. The effective adsorption process of CRLE on activated carbon attributed to its porous structure and the presence of various functional groups on its surface. The study of the effect of the process variables showed that the adsorption process was highly dependent on the initial CRLE concentration, the temperature, the solution pH, and the ionic strength. In this study, the maximum adsorption capacity of CRLE on activated carbon was found at pH of 5.5. The highest adsorption parameters of CRLE on active carbon were found to be 96.2 mg/g at pH 5.5, 309.5 K, and initial enzyme concentration of 5.0×10^{-3} M, respectively. The values of free Gibbs energy were found as negative that shows the adsorption process of CRLE on activated carbon occurs spontaneously. Additionally, Gibbs energy values indicate the adsorption process is a physical process. Based on the result, we can say that activated carbon can be effectively used as an adsorbent for the adsorption of CRLE.

References

1. Daşdelen, Z., Yıldız, Y., Eriş, S., & Şen, F. (2017). Enhanced electrocatalytic activity and durability of Pt nanoparticles decorated on GO-PVP hybrid material for methanol oxidation reaction. *Applied Catalysis B: Environmental, 219*, 511–516. https://doi.org/10.1016/j.apcatb.2017.08.014.
2. Bozkurt, S., Tosun, B., Sen, B., Akocak, S., Savk, A., Ebeoğlugil, M. F., & Sen, F. (2017). A hydrogen peroxide sensor based on TNM functionalized reduced graphene oxide grafted with highly monodisperse Pd nanoparticles. *Analytica Chimica Acta, 989*, 88–94. https://doi.org/10.1016/j.aca.2017.07.051.
3. Goksu, H., Sert, H., Kilbas, B., & Sen, F. (2017). Recent advances in the reduction of nitro compounds by heterogenous catalysts. *Current Organic Chemistry, 21*, 794–820. https://doi.org/10.2174/1385272820666160525123907.
4. Demirbaş Ö., Çalımlı M.H., Kuyuldar E., Halil B.İ., Nas M.S., Şen F. (2019) Thermodynamic kinetics and sorption of bovine serum albumin with different clay materials. In: Inamuddin (eds) applications of ion exchange materials in biomedical industries. Springer, Cham. doi.org/10.1007/978-3-030-06082-4_6.
5. Aday, B., Pamuk, H., Kaya, M., & Sen, F. (2016). Graphene oxide as highly effective and readily recyclable catalyst using for the one-pot synthesis of 1,8-dioxoacridine derivatives. *Journal of Nanoscience and Nanotechnology, 16*, 6498–6504. https://doi.org/10.1166/jnn.2016.12432.
6. Eris, S., Daşdelen, Z., & Sen, F. (2018). Enhanced electrocatalytic activity and stability of monodisperse Pt nanocomposites for direct methanol fuel cells. *Journal of Colloid and Interface Science, 513*, 767–773. https://doi.org/10.1016/j.jcis.2017.11.085.
7. Akocak, S., Şen, B., Lolak, N., Şavk, A., Koca, M., Kuzu, S., & Şen, F. (2017). One-pot three-component synthesis of 2-amino-4H-chromene derivatives by using monodisperse Pd nanomaterials anchored graphene oxide as highly efficient and recyclable catalyst. *Nano-Structures & Nano-Objects, 11*, 25–31. https://doi.org/10.1016/j.nanoso.2017.06.002.
8. Demirbas, O., Calimli, M.H., Kuyuldar, E. et al. (2019) Equilibrium, kinetics, and thermodynamic of adsorption of enzymes on diatomite clay materials. BioNanoScience. https://doi.org/10.1007/s12668-019-00615-1.
9. Erken, E., Pamuk, H., Karatepe, Ö., Başkaya, G., Sert, H., Kalfa, O. M., & Şen, F. (2016). New Pt(0) nanoparticles as highly active and reusable catalysts in the C1–C3 alcohol oxidation and the room temperature dehydrocoupling of dimethylamine-borane (DMAB). *Journal of Cluster Science, 27*, 9–23. https://doi.org/10.1007/s10876-015-0892-8.
10. Ayranci, R., Başkaya, G., Güzel, M., Bozkurt, S., Şen, F., & Ak, M. (2017). Carbon based nanomaterials for high performance optoelectrochemical systems. *ChemistrySelect, 2*, 1548–1555. https://doi.org/10.1002/slct.201601632.
11. Çalımlı, M. H., Demirbaş, Ö., Aygün, A., et al. (2018). Immobilization kinetics and mechanism of bovine serum albumin on diatomite clay from aqueous solutions. *Applied Water Science, 8*, 209. https://doi.org/10.1007/s13201-018-0858-8.
12. Karatepe, Ö., Yıldız, Y., Pamuk, H., Eris, S., Dasdelen, Z., & Sen, F. (2016). Enhanced electrocatalytic activity and durability of highly monodisperse Pt@PPy–PANI nanocomposites as a novel catalyst for the electro-oxidation of methanol. *RSC Advances, 6*, 50851–50857. https://doi.org/10.1039/C6RA06210E.
13. Şen, F., Demirbaş, Ö., Çalımlı, M. H., et al. (2018). The dye removal from aqueous solution using polymer composite films. *Applied Water Science, 8*, 206. https://doi.org/10.1007/s13201-018-0856-x.
14. Abrahamson, J. T., Sempere, B., Walsh, M. P., Forman, J. M., Şen, F., Şen, S., Mahajan, S. G., Paulus, G. L. C., Wang, Q. H., Choi, W., & Strano, M. S. (2013). Excess thermopower and the theory of thermopower waves. *ACS Nano, 7*, 6533–6544. https://doi.org/10.1021/nn402411k.
15. Demirbaş, Ö., & Nas, M. S. (2016). Kinetics and mechanism of the adsorption of methylene blue from aqueous solution onto Turkish green clay. *Archives of Current Research International, 6*(3), 1–10. https://doi.org/10.9734/ACRI/2016/30677.
16. Bujdák, J., & Rode, B. M. (1997). Silica, alumina, and clay-catalyzed alanine peptide bond formation. *Journal of Molecular Evolution, 45*, 457–466. https://doi.org/10.1007/PL00006250.
17. Bujdák, J., Le, S. H., & Rode, B. M. (1996). Montmorillonite catalyzed peptide bond formation: the effect of exchangeable cations. *Journal of Inorganic Biochemistry, 63*, 119–124. https://doi.org/10.1016/0162-0134(95)00186-7.
18. Causserand, C., Jover, K., Aimar, P., & Meireles, M. (1997). Modification of clay cake permeability by adsorption of protein. *J Memb Sci, 137*, 31–44. https://doi.org/10.1016/S0376-7388(97)00181-6.
19. Ding, X., & Henrichs, S. M. (2002). Adsorption and desorption of proteins and polyamino acids by clay minerals and marine

sediments. *Marine Chemistry, 77*, 225–237. https://doi.org/10.1016/S0304-4203(01)00085-8.

20. Fusi, P., Ristori, G. G., Calamai, L., & Stotzky, G. (1989). Adsorption and binding of protein on "clean" (homoionic) and "dirty" (coated with Fe oxyhydroxides) montmorillonite, illite and kaolinite. *Soil Biology and Biochemistry, 21*, 911–920. https://doi.org/10.1016/0038-0717(89)90080-1.
21. Gupta, A., Loew, G. H., & Lawless, J. (1983). Interaction of metal ions and amino acids: possible mechanisms for the adsorption of amino acids on homoionic smectite clays. *Inorganic Chemistry, 22*, 111–120. https://doi.org/10.1021/ic00143a025.
22. Quiquampoix, H., Staunton, S., Baron, M. H., & Ratcliffe, R. G. (1993). Interpretation of the pH dependence of protein adsorption on clay mineral surfaces and its relevance to the understanding of extracellular enzyme activity in soil. *Colloids and Surfaces A: Physicochemical and Engineering Aspects, 75*, 85–93. https://doi.org/10.1016/0927-7757(93)80419-F.
23. Rigou, P., Rezaei, H., Grosclaude, J., Staunton, S., & Quiquampoix, H. (2006). Fate of prions in soil: adsorption and extraction by electroelution of recombinant ovine prion protein from montmorillonite and natural soils. *Environmental Science & Technology, 40*, 1497–1503. https://doi.org/10.1021/es0516965.
24. Violante, A. (1995). Physicochemical properties of protein-smectite and protein-Al(OH)x-smectite complexes. *Clay Minerals, 30*, 325–336. https://doi.org/10.1180/claymin.1995.030.4.06.
25. Schmid, R. D., & Verger, R. (1998). Lipases: interfacial enzymes with attractive applications. *Angewandte Chemie International Edition, 37*, 1608–1633. https://doi.org/10.1002/(SICI)1521-3773(19980703)37:12<1608::AID-ANIE1608>3.0.CO;2-V.
26. Albertsson, A., & Srivastava, R. (2008). Recent developments in enzyme-catalyzed ring-opening polymerization☆. *Advanced Drug Delivery Reviews, 60*, 1077–1093. https://doi.org/10.1016/j.addr.2008.02.007.
27. Gitlesen, T., Bauer, M., & Adlercreutz, P. (1997). Adsorption of lipase on polypropylene powder. *Biochimica et Biophysica Acta, Lipids and Lipid Metabolism, 1345*, 188–196. https://doi.org/10.1016/S0005-2760(96)00176-2.
28. Cao, L. (2005) Carrier-bound immobilized enzymes. doi: https://doi.org/10.1002/3527607668.
29. Yu, W. H., Li, N., Tong, D. S., Zhou, C. H., Lin, C. X., & Xu, C. Y. (2013). Adsorption of proteins and nucleic acids on clay minerals and their interactions: a review. *Applied Clay Science, 80–81*, 443–452. https://doi.org/10.1016/j.clay.2013.06.003.
30. Blanco, R. M., Terreros, P., Fernández-Pérez, M., et al. (2004). Functionalization of mesoporous silica for lipase immobilization. *Journal of Molecular Catalysis B: Enzymatic, 30*, 83–93. https://doi.org/10.1016/j.molcatb.2004.03.012.
31. Hook, F., Rodahl, M., Kasemo, B., & Brzezinski, P. (1998). Structural changes in hemoglobin during adsorption to solid surfaces: effects of pH, ionic strength, and ligand binding. *Proceedings of the National Academy of Sciences, 95*, 12271–12276. https://doi.org/10.1073/pnas.95.21.12271.
32. Oliva, F. Y., Avalle, L. B., Cámara, O. R., & De Pauli, C. P. (2003). Adsorption of human serum albumin (HSA) onto colloidal TiO2 particles, part I. *Journal of Colloid and Interface Science, 261*, 299–311. https://doi.org/10.1016/S0021-9797(03)00029-8.
33. Sternik, D., Staszczuk, P., Grodzicka, G., Pękalska, J., & Skrzypiec, K. (2004). Studies of physicochemical properties of the surfaces with the chemically bonded phase of BSA. *Journal of Thermal Analysis and Calorimetry, 77*, 171–182. https://doi.org/10.1023/B:JTAN.0000033201.86803.fa.
34. Vroman, L., & Adams, A. L. (1969). Findings with the recording ellipsometer suggesting rapid exchange of specific plasma proteins at liquid/solid interfaces. *Surface Science, 16*, 438–446. https://doi.org/10.1016/0039-6028(69)90037-5.
35. Aygün, A., Yenisoy-Karakaş, S., & Duman, I. (2003). Production of granular activated carbon from fruit stones and nutshells and evaluation of their physical, chemical and adsorption properties. *Microporous and Mesoporous Materials, 66*, 189–195. https://doi.org/10.1016/j.micromeso.2003.08.028.
36. Rajeshwarisivaraj, Sivakumar, S., Senthilkumar, P., & Subburam, V. (2001). Carbon from cassava peel, an agricultural waste, as an adsorbent in the removal of dyes and metal ions from aqueous solution. *Bioresource Technology, 80*, 233–235. https://doi.org/10.1016/S0960-8524(00)00179-6.
37. Avom, J., Mbadcam, J. K., Noubactep, C., & Germain, P. (1997). Adsorption of methylene blue from an aqueous solution on to activated carbons from palm-tree cobs. *Carbon N Y, 35*, 365–369. https://doi.org/10.1016/S0008-6223(96)00158-3.
38. El-Sheikh, A. H., Newman, A. P., Al-Daffaee, H. K., Phull, S., & Cresswell, N. (2004). Characterization of activated carbon prepared from a single cultivar of Jordanian olive stones by chemical and physicochemical techniques. *Journal of Analytical and Applied Pyrolysis, 71*, 151–164. https://doi.org/10.1016/S0165-2370(03)00061-5.
39. Wu, F. (1999). Pore structure and adsorption performance of the activated carbons prepared from plum kernels. *Journal of Hazardous Materials, 69*, 287–302. https://doi.org/10.1016/S0304-3894(99)00116-8.
40. Tsai, W., Chang, C., Lin, M., Chien, S., Sun, H., & Hsieh, M. (2001). Adsorption of acid dye onto activated carbons prepared from agricultural waste bagasse by ZnCl2 activation. *Chemosphere, 45*, 51–58. https://doi.org/10.1016/S0045-6535(01)00016-9.
41. Senthilkumaar, S., Varadarajan, P. R., Porkodi, K., & Subbhuraam, C. V. (2005). Adsorption of methylene blue onto jute fiber carbon: kinetics and equilibrium studies. *Journal of Colloid and Interface Science, 284*, 78–82. https://doi.org/10.1016/j.jcis.2004.09.027.
42. Yalçın, N., & Sevinç, V. (2000). Studies of the surface area and porosity of activated carbons prepared from rice husks. *Carbon N Y, 38*, 1943–1945. https://doi.org/10.1016/S0008-6223(00)00029-4.
43. Girgis, B. S., & El-Hendawy, A.-N. A. (2002). Porosity development in activated carbons obtained from date pits under chemical activation with phosphoric acid. *Microporous and Mesoporous Materials, 52*, 105–117. https://doi.org/10.1016/S1387-1811(01)00481-4.
44. Chang, Y. K., Chu, L., Tsai, J. C., & Chiu, S. J. (2006). Kinetic study of immobilized lysozyme on the extrudate-shaped NaY zeolite. *Process Biochemistry, 41*, 1864–1874. https://doi.org/10.1016/j.procbio.2006.03.039.
45. https://www.tarimbilgisi.com, date of access:23.09.2018.
46. Amuda, O. S., Giwa, A. A., & Bello, I. A. (2007). Removal of heavy metal from industrial wastewater using modified activated coconut shell carbon. *Biochemical Engineering Journal, 36*, 174–181. https://doi.org/10.1016/j.bej.2007.02.013.
47. Guo, Y., & Bustin, R. (1998). FTIR spectroscopy and reflectance of modern charcoals and fungal decayed woods: implications for studies of inertinite in coals. *International Journal of Coal Geology, 37*, 29–53. https://doi.org/10.1016/S0166-5162(98)00019-6.
48. Figueiredo, J., Pereira, M. F., Freitas, M. M., & Órfão, J. J. (1999). Modification of the surface chemistry of activated carbons. *Carbon N Y, 37*, 1379–1389. https://doi.org/10.1016/S0008-6223(98)00333-9.
49. Natalello, A., Ami, D., Brocca, S., Lotti, M., & Doglia, S. M. (2005). Secondary structure, conformational stability and glycosylation of a recombinant Candida rugosa lipase studied by Fourier-transform infrared spectroscopy. *The Biochemical Journal, 385*, 511–517. https://doi.org/10.1042/BJ20041296.
50. Vinu, A., Murugesan, V., & Hartmann, M. (2004). Adsorption of lysozyme over mesoporous molecular sieves MCM-41 and SBA-

15: influence of pH and aluminum incorporation. *The Journal of Physical Chemistry. B, 108*, 7323–7330. https://doi.org/10.1021/jp037303a.
51. Sreeramamurthy, R., & Menon, P. G. (1975). Oxidation of H2S on active carbon catalyst. *Journal of Catalysis, 37*, 287–296.
52. Reshmi R.S.S. (2007) Immobilization and characteristics of Candida rugosa lipase onto siliceous mesoporous molecular sieves and montmorillonite K-10 for synthesis of flavour esters. In: Proc. Int. Conf. Adv. Mater. Compos. India: NIIST, pp 819–824.
53. Tekin, N., Demirbaş, Ö., & Alkan, M. (2005). Adsorption of cationic polyacrylamide onto kaolinite. *Microporous and Mesoporous Materials, 85*, 340–350. https://doi.org/10.1016/j.micromeso.2005.07.004.
54. Vermöhlen, K., Lewandowski, H., Narres, H. D., & Schwuger, M. (2000). Adsorption of polyelectrolytes onto oxides — the influence of ionic strength, molar mass, and Ca2+ ions. *Colloids and Surfaces A: Physicochemical and Engineering Aspects, 163*, 45–53. https://doi.org/10.1016/S0927-7757(99)00429-X.
55. Dalla, V. R., Sebrão, D., Nascimento, M., & Soldi, V. (2005). Carboxymethyl cellulose and poly(vinyl alcohol) used as a film support for lipases immobilization. *Process Biochemistry, 40*, 2677–2682. https://doi.org/10.1016/j.procbio.2004.12.004.
56. Pronk, W., Kerkhof, P., Van Helden, C., & van'T Riet, K. (1988). The hydrolysis of triglycerides by immobilized lipase in a hydrophiiic membrane reactor. *Biotechnology and Bioengineering, 32*, 512–518. https://doi.org/10.1002/bit.260320414.
57. Gregory, J. (1994) Introduction to modern colloid science, Robert J. Hunter. Oxford University press, Oxford, 1993. Pp. viii + 338, price £14.95 (paperback). ISBN 0-19-855386-2. Polymer International 35:105–106. doi: https://doi.org/10.1002/pi.1994.210350115.
58. Doğan, M., Alkan, M., Demirbaş, Ö., Özdemir, Y., & Özmetin, C. (2006). Adsorption kinetics of maxilon blue GRL onto sepiolite from aqueous solutions. *Chemical Engineering Journal, 124*, 89–101. https://doi.org/10.1016/j.cej.2006.08.016.
59. Lee, D. C., & Chapman, D. (1986). Infrared spectroscopic studies of biomembranes and model membranes. *Bioscience Reports, 6*, 335–356.
60. Demirbas, O. (2006) Methyl violetine biosorption on casein surface.
61. Ho, Y., & McKay, G. (1999). The sorption of lead(II) ions on peat. *Water Research, 33*, 578–584. https://doi.org/10.1016/S0043-1354(98)00207-3.
62. Ozturk, N., & Kavak, D. (2005). Adsorption of boron from aqueous solutions using fly ash: batch and column studies. *Journal of Hazardous Materials, 127*, 81–88. https://doi.org/10.1016/j.jhazmat.2005.06.026.
63. Aharoni, C., Sideman, S., & Hoffer, E. (2007). Adsorption of phosphate ions by collodion-coated alumina. *Journal of Chemical Technology and Biotechnology, 29*, 404–412. https://doi.org/10.1002/jctb.503290703.
64. Ho, Y. S., & McKay, G. (1998). Sorption of dye from aqueous solution by peat. *Chemical Engineering Journal, 70*, 115–124. https://doi.org/10.1016/S0923-0467(98)00076-1.
65. Basyaruddin, M., Rahman, A., Basri, M., Hussein, M. Z., et al. (2003). Activated carbon as support for lipase immobilization. *Eurasian ChemTech Journal, 5*, 115–119.
66. Fagain, C.O. (1997) Manipulating protein stability in stabilizing proteins functions, Heidelberg, Berlin, Springer, New York. 67.
67. Karthikeyan, T., Rajgopal, S., & Miranda, L. (2005). Chromium(VI) adsorption from aqueous solution by sawdust activated carbon. *Journal of Hazardous Materials, 124*, 192–199. https://doi.org/10.1016/j.jhazmat.2005.05.003.
68. Bhattacharya, A., Naiya, T., Mandal, S., & Das, S. (2007). Adsorption, kinetics and equilibrium studies on removal of Cr(VI) from aqueous solutions using different low-cost adsorbents. *Chemical Engineering Journal, 137*, 529–541. https://doi.org/10.1016/j.cej.2007.05.021.
69. Sharma, Y. C. (2001). Effect of temperature on interfacial adsorption of Cr(VI) on Wollastonite. *Journal of Colloid and Interface Science, 233*, 265–270. https://doi.org/10.1006/jcis.2000.7232.
70. Sariri, R. B. T. (1996). Effect of surface chemistry on protein interaction with hydrogel contact lenses. *Iranian Polymer Journal, 5*, 266.
71. Xu, H., Li, M., & He, B. (1995). Immobilization of Candida cylindracea lipase on methyl acrylate-divinyl benzene copolymer and its derivatives. *Enzyme and Microbial Technology, 17*, 194–199. https://doi.org/10.1016/0141-0229(94)00038-S.
72. Lian, L., Guo, L., & Guo, C. (2009). Adsorption of Congo red from aqueous solutions onto ca-bentonite. *Journal of Hazardous Materials, 161*, 126–131. https://doi.org/10.1016/j.jhazmat.2008.03.063.
73. Montero, S., Blanco, A., Virto, M. D., Carlos, L. L., Agud, I., Solozabal, R., Lascaray, J., de Renobales, M., Llama, M. J., & Serra, J. L. (1993). Immobilization of Candida rugosa lipase and some properties of the immobilized enzyme. *Enzyme and Microbial Technology, 15*, 239–247. https://doi.org/10.1016/0141-0229(93)90144-Q.
74. Guncheva, M., Paunova, K., Dimitrov, M., & Yancheva, D. (2014). Stabilization of *Candida rugosa* lipase on nanosized zirconia-based materials. *Journal of Molecular Catalysis B: Enzymatic, 108*, 43–50.
75. Demiral, H., Demiral, İ., Tümsek, F., & Karabacakoğlu, B. (2008). Adsorption of chromium(VI) from aqueous solution by activated carbon derived from olive bagasse and applicability of different adsorption models. *Chemical Engineering Journal, 144*, 188–196. https://doi.org/10.1016/j.cej.2008.01.020.
76. Salis, A., Cugia, F., Setzu, S., Mula, G., & Monduzzi, M. (2010). Effect of oxidation level of n+ type mesoporous silicon surface on the adsorption and the catalytic activity of *Candida rugosa* lipase. *Journal of Colloid and Interface Science, 345*, 448–453.
77. Lu, P., & Hsieh, Y. L. (2009). Lipase bound cellulose nanofibrous membrane via cibacron blue F3GA affinity ligand. *Journal of Membrane Science, 330*, 288–296.
78. Amirkhani, L., Moghaddas, J., & Malmiri, H. J. (2016). Candida rugosa lipase immobilization on magnetic silica aerogel nanodispersion. *RSC Advances, 6*, 12676–12687.
79. Alves, M., Aracri, F., Cren, É., & Mendes, A. (2017). Isotherm, kinetic, mechanism and thermodynamic studies of adsorption of a microbial lipase on a mesoporous and hydrophobic resin. *Chemical Engineering Journal, 311*, 1–12.